JOURNAL OF VIROLOGY, May 2005, p. 5996–6004 Vol. 79, No. 10
0022-538X/05/$08.00+0 doi:10.1128/JVI.79.10.5996–6004.2005

Amino Acid 36 in the Human Immunodeficiency Virus Type 1 gp41 Ectodomain Controls Fusogenic Activity: Implications for the Molecular Mechanism of Viral Escape from a Fusion Inhibitor

Masanobu Kinomoto,[1,3] Masaru Yokoyama,[2] Hironori Sato,[2] Asato Kojima,[1] Takeshi Kurata,[1] Kazuyoshi Ikuta,[3] Tetsutaro Sata,[1] and Kenzo Tokunaga[1]*

Department of Pathology[1] and Division of Molecular Genetics,[2] National Institute of Infectious Diseases, Tokyo 162-8640, and Department of Virology, Research Institute for Microbial Diseases, Osaka University, Osaka 565-0871,[3] Japan

Received 29 October 2004/Accepted 6 January 2005

We have previously described a human immunodeficiency virus type 1 (HIV-1) proviral clone, pL2, derived from defective viral particles with higher fusogenicity than the prototypic NL4-3 virus. In this study, we attempted to determine the region that confers the enhanced fusion activity by creating envelope recombinants between pL2 and pNL4-3, as well as point mutants based on pNL4-3. The results indicate that amino acid 36 of gp41 is key for the fusogenic activity and infectivity enhancement and that glycine 36 (36G) of gp41 in pL2 is conserved in nearly all HIV-1 isolates except for pNL4-3. The mutation 36G→D in a primary-isolate-derived Env decreased syncytium-forming activity and infectivity. The assays for cell-cell fusion and viral binding suggested that the enhanced fusion mediated by the 36D→G mutation is not due to increased binding efficiency but is directly due to actual enhancement of viral fusion activity. Interestingly, this amino acid position is exactly equivalent to that at which the mutation of HIV-1 isolates that have escaped from a fusion inhibitor, enfuvirtide (T-20), has been frequently observed. The correlation between these previous findings and our findings was suggested by structural analysis. Our finding, therefore, has implications for a molecular basis of the viral escape from this drug.

The human immunodeficiency virus type 1 (HIV-1) envelope glycoprotein (Env), which determines viral tropism, is initially synthesized as a single polypeptide precursor, gp160, forming trimers (46). Subsequently, this Env precursor is cleaved proteolytically into a heavily glycosylated surface subunit known as gp120 and a transmembrane subunit known as gp41, which are associated by noncovalent bonds in an oligomeric structure on the surface of the virion (10, 18, 31). On the target cell surface, the gp120 surface protein binds to CD4 and a coreceptor, leading to a conformational change in gp120 that alters gp120-gp41 interactions (23, 47). This binding event triggers membrane fusion, which requires functions of gp41 ectodomain. The gp41 ectodomain contains a hydrophobic amino-terminal fusion peptide, followed by an amino-terminal and carboxy-terminal leucine/isoleucine heptad repeat domain with a helical structure (N-peptide helix and C-peptide helix, respectively) (3, 6, 26, 36, 43). Fusion is first induced by insertion of the fusion peptide at the amino terminus of gp41 into the host cell membrane, after which this region is brought into close proximity to the transmembrane domain of gp41. This is attained via the fusion-active conformation of a coiled-coil structure composed of internal triple-stranded N-peptide helices paired with antiparallel outer C-peptide helices packed along hydrophobic grooves, thus forming a six-helix bundle (7, 43).

The fusion inhibitor enfuvirtide (also known as T-20), a peptide based on the sequence of the C-peptide helix in gp41, blocks formation of the six-helix bundle and thus prevents membrane fusion (8, 27, 45). A mutation in the N-peptide helix of gp41, specifically, an aspartic acid substitution for glycine at position 36, which was selected both in vitro (24, 35, 40) and in vivo (42), affects viral sensitivity to T-20, presumably by altering the affinity of T-20 for the N-peptide helix.

We have previously reported that an established cell line, L-2, derived from MT-4 cells surviving after in vitro acute-phase infection with an MT-4/MOLT-4 cell-propagated LAI strain, produces highly fusogenic but replication-defective HIV-1 particles (20). The L-2-produced viruses are peculiar, as the morphology of the viral particles is doughnut shaped since the protease gene is mutated and in that the virions harbor a robust activity to induce syncytia despite lacking infectivity (16, 32). To characterize the L-2-derived viruses, we generated a full-length infectious DNA clone, pL2, using proviral DNA extracted from L-2 cells. By performing a chimeric analysis between pL2 and pNL4-3, we found that pL2-derived regions, including *env*, induce enhanced syncytium formation as expected (21).

In this study, we further sought to determine the region that conferred the fusogenic activity at the amino acid level, by creating *env* recombinants between pL2 (or its parent pLAI) and pNL4-3, and several point mutants based on pNL4-3. The results demonstrate that amino acid 36 of gp41 is a key deter-

* Corresponding author. Mailing address: Department of Pathology, National Institute of Infectious Diseases, 1-23-1 Toyama, Shinjuku-ku, Tokyo 162-8640, Japan. Phone: 81 3 5285 1111. Fax: 81 3 5285 1189. E-mail: tokunaga@nih.go.jp.

minant of the fusion activity and infectivity enhancement and that glycine 36 of gp41, commonly seen in pL2 and the parental pLAI, is conserved in nearly all HIV-1 isolates except for pNL4-3 (and, surprisingly, T-20 escape mutants), which carry aspartic acid at this position (36D). By exploiting structural modeling of gp41, we were able to predict the cause of the fusogenic difference between L2/LAI and NL4-3 viruses. Together with the finding that escape mutants from the T-20 fusion inhibitor harbor the same 36D mutation (24, 27, 35, 40, 42), these results imply a molecular basis for the emergence of viruses resistant to this drug.

MATERIALS AND METHODS

Plasmid construction. To introduce a unique restriction enzyme site at the 3′ end of the envelope gene, a PCR-amplified BamHI-NotI fragment (nucleotide positions 8465 to 8786) and an amplified NotI-XhoI fragment (positions 8787 to 8887) from pNL4-3 (1) were ligated into pNL4-3 digested with BamHI and XhoI restriction enzymes (pNL-e-Not). To further introduce unique restriction enzyme sites into an *env* sequence, the SalI-NotI fragment (positions 5785 to 8786) of pNL-e-Not was subcloned into pBlueScript SK(+) (Stratagene) (pBS-NL-S/N). MroI and BlpI sites were introduced immediately upstream of the envelope signal peptide sequence (positions 6214 to 6219) and cleavage signal sequence (positions 7715 to 7721), respectively, on pBS-NL-S/N, and this construct was designated pBSNL-S/N-M/B. The SalI-NotI region of pBSNL-S/N-M/B was cloned back into pNL-e-Not to create pNL-envCT. An envelope gp41-coding sequence derived from pLAI was PCR amplified and inserted into pNL-envCT, to generate the proviral clone pNL-LAIgp41. An envelope gp120 sequence from pLAI was also PCR amplified and subcloned into MroI- and BlpI-digested pBSNL-S/N-M/B, and then the SalI-BlpI fragment was replaced with either pNL-LAIgp41 or pNL-envCT, to generate the proviral clone pNL-LAIgp160 or pNL-LAIgp120, respectively. In order to generate more recombinants of gp41, the NheI (positions 7250 to 7255)-XhoI (positions 8887 to 8892) fragment of pNL-envCT was inserted into a pGL3-Basic vector (Promega) and designated pGL3NL-N/X-Blp. Either the BlpI-HindIII (positions 7715 to 8136) or HindIII-BamHI (positions 8131 to 8470) fragment derived from pLAI was inserted into pGL3NL-N/X-Blp. The BlpI-NotI fragment of each plasmid carrying either BlpI-HindIII or HindIII-BamHI of pLAI was inserted back into pNL-envCT to create pNL-LAIgp41-1 and pNL-LAIgp41-2, respectively. To generate the proviral clone pNL-LAIgp41-3, a PCR-amplified BamHI-NotI fragment of pLAI was directly inserted into pNL-envCT. Chimeric proviral clones carrying pL2-derived sequence were also constructed by using the same strategies. These proviral clones were designated pNL-L2gp160, pNL-L2gp120, pNL-L2gp41, pNL-L2gp41-1, pNL-L2gp41-2, and pNL-L2gp41-3. To introduce the amino acid mutation 21Cys→Ala, 22Thr→Arg, 36Asp→Gly, 22Thr→Ala, or 91Leu→Phe, QuikChange mutagenesis (Stratagene) was performed by using pGL3NL-N/X-Blp as a template DNA. The resultant BlpI and NotI fragments were inserted into pNL-envCT, and the constructs were designated pNL-gp41-C21A, pNL-gp41-T22R, pNL-gp41-T22A, pNL-gp41-D36G, and pNL-gp41-L91F, respectively. Similarly, an amino acid change of 36Gly→Asp was introduced into pNL-1549 harboring a primary isolate (QH1549)-derived Env protein (37) to create pNL-1549-G36D. To quantify the infectivity, the PCR-amplified NotI-XhoI fragment of the luciferase (Luc) gene was inserted into NotI-XhoI region of pNL-envCT, pNL-gp41-D36G, pNL-1549, or pNL-1549-G36D and designated pNL-Luc-envCT, pNL-Luc-gp41-D36G, pNL-Luc-1549, or pNL-Luc-1549-G36D, respectively. Env expression plasmids pNLnΔBs (NL-Env expression plasmid) and pNLnΔBs-Nh (ΔEnv control plasmid) were previously described (38). pNLnΔBs-D36G was constructed by replacement of the NheI-BamHI region of pNL-gp41-D36G in the corresponding sites of pNLnΔBs. To generate pLTR-hLucP+, the 5′ long terminal repeat (LTR) sequence of pNL4-3 was PCR amplified and inserted into pGL3(R2.1)-Basic vector carrying the Rapid Response luciferase gene (Promega). To generate a Tat expression plasmid, pLTR-Tat, the *tat* sequence of pNL4-3 was PCR amplified and replaced with the humanized Luc gene from pLTR-hLucP+. To generate pNL-Δenv, an envelope-defective control vector, a frameshift mutation was introduced into the NdeI site within *env* gene of pNL4-3.

Cell maintenance and transfection. MOLT-4, M8166, CEMx174, H9, 293T, and MAGIC5A cells were maintained as described elsewhere (30, 32, 38). To prepare viral supernatants, 7×10^5 293T cells were transfected with 2 μg of each proviral expression plasmid by using FuGENE 6 (Roche). Sixteen hours later, cells were washed with phosphate-buffered saline (PBS), and then 2 ml of fresh complete medium was added. Twenty-four hours later, supernatants were filtered through 0.45-μm-pore-size filters. Levels of virion production were quantitated by HIV-1 p24 antigen capture enzyme-linked immunosorbent assay (ELISA) (Retro-Tek).

Syncytium formation assay. MOLT-4, M8166, CEMx174, or H9 cells (5×10^4) were incubated with 200 ng of p24 antigen of each virus at 37°C. After incubation for 48 h, the cells were fixed with 4% paraformaldehyde in PBS, and the formation of syncytia was observed under a light microscope.

Viral infectivity assay. MAGIC5A cells (5×10^5) were incubated with viral supernatants containing 10 ng of p24 antigen. Forty-eight hours after infection, cells were lysed in 100 μl of lysis buffer (Promega), and Luc activities were measured by MicroLumat LB 96V (Berthold).

Viral binding assay. One hundred nanograms of p24 of NL-Δenv (control), NL-envCT (wild type [WT]), or NL-gp41-D36G (D36G mutant) virus was added to 1.5×10^6 MAGIC5A cells at 4°C. After 3 h of incubation, cells were washed three times with PBS and then lysed in 100 μl of lysis buffer. The p24 antigen content of the lysates was measured by ELISA. The background obtained with control viruses was subtracted from sample values.

Cell-cell fusion assay. 293T cells as effector cells and MAGIC5A cells as target cells were transfected with pNLnΔBs (WT-env), pNLnΔBs-D36G (D36G-env), or pNLnΔBs-Nh (control env), plus pLTR-Tat, and with pLTR-hLucP+, respectively. After 48 h, both cell types were washed, trypsinized, and cocultured in a 12-well plate. After 5 h of incubation, cells were lysed in 200 μl of lysis buffer, and Luc activities were measured with a MicroLumat LB 96V. Transfection efficiency was normalized by cotransfection of 293T with phRL-CMV (Promega), which expresses a renilla luciferase.

Molecular modeling of the HIV-1 gp41 ectodomain trimer. To construct three-dimensional (3-D) structures of intact ectodomain trimers, we used the crystal structure of the simian immunodeficiency virus gp41 ectodomain trimer at a high resolution at 1.47 Å (Protein Data Bank code 1QBZ) (48) as a template for homology modeling. Although several other crystallographic structures of the HIV-1 gp41 ectodomain are available from the Protein Data Bank, those structures are either monomers or trimers lacking a majority of the N helix, C helix, and loop connecting the helices. 1QBZ has a sequence similarity of 52.5% to the target NL4-3 gp41 ectodomain, which is high enough to construct high-accuracy models with a root mean square distance (RMSD) of ~1 Å for the main chain between the predicted and actual structures (2). Monomer chains termed A, B, and C in the trimer structure 1QBZ lack 21, 9, and 3 amino acid residues, respectively. To minimize effects of the missing residues on the modeling, 1QBZ was modified by superimposing the chain C residues, which carry the fewest missing residues, on the chain A and chain B residues, and the modified 1QBZ structure was used as a template structure for modeling. 3-D models of HIV-1 gp41 ectodomain trimers of NL4-3 and the D36G mutant were constructed independently by the homology modeling technique using MOE-Align and MOE-Homology in the Molecular Operating Environment (MOE) (Chemical Computing Group Inc.). The 3-D structures were thermodynamically optimized by energy minimization using the MOE and a CHARMm22 force field. Physically unacceptable local structures of the optimized 3-D models were further refined on the basis of evaluation by Ramachandran plot and chi plot using programs packaged in MOE. We also tested distinct procedure for the modeling. In this case, we first made the NL4-3 gp41 model alone from the simian immunodeficiency virus template structure and then substituted the amino acid at position 36 from D to G, followed by energy minimization. This procedure generated a structure indistinguishable from the D36G structure obtained by the first procedure. Thus, we used structures made by the first procedure in the present study.

RESULTS

Ability of envelope gp120- and gp41-chimeric viruses to form syncytia. We first constructed a cassette vector, pNL-envCT, for envelope recombination. pLAI- and pL2-derived gp160 fragments were PCR amplified and cloned into pNL-envCT to generate pNL-LAIgp160 and pNL-L2gp160. The resultant chimeric viruses carrying the entire gp160 envelopes of pLAI and pL2 were analyzed in a syncytium formation assay. As expected, full-length Envs from pLAI and pL2 were fully able to support high-level fusion activity (Fig. 1), while NL4-3 Env did not reveal such a fusion activity under our experimental conditions. Since a significant number of reports

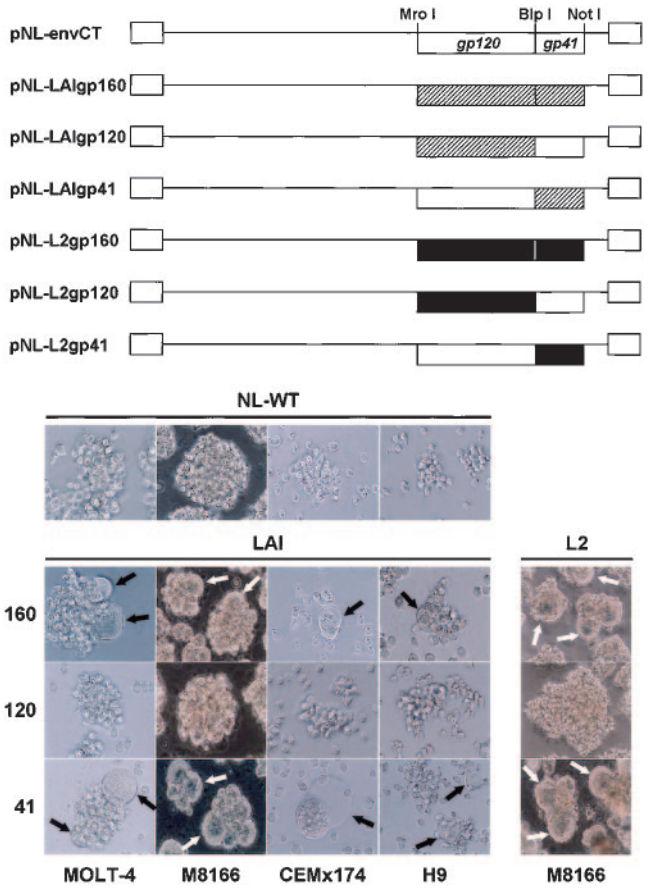

FIG. 1. Construction of gp120 and gp41 chimeric full-length proviral DNAs and their syncytium-forming activities. An HIV-1 envelope cassette vector, pNL-envCT (WT), harbors MroI, BlpI, and NotI restriction enzyme sites immediately upstream of the gp120, gp41, and *nef* genes of pNL4-3, respectively. The envelope gp160, gp120, and gp41 genes of pLAI and pL2 were replaced with the corresponding regions of pNL-envCT. MOLT-4, M8166, CEMx174, or H9 cells (5×10^4) were incubated with 200 ng of p24 antigen of each virus. After 48 h, cells were fixed and observed by microscopy. Arrows indicate the formation of syncytia.

regarding the role of gp41 envelope in fusogenic activity have been accumulated (4, 5, 12, 15, 19, 33), we attempted to assess whether pLAI- and pL2-derived gp41 could indeed determine the ability to induce high fusogenic activity. The gp120 or gp41 region derived from pLAI or pL2 was cloned in place of the equivalent *env* sequence present in pNL-envCT, and the abilities of these envelope-chimeric HIV-1 proviral clones to induce fusion activity were analyzed. As shown in Fig. 1, NL-LAIgp41 and NL-L2gp41 revealed high fusion activity similar to that observed in NL-LAIgp160 and NL-L2gp160, while NL-LAIgp120 and NL-L2gp120 did not show any syncytium formation. Therefore, we conclude that pLAI- and pL2-derived gp41 envelopes indeed determine the ability to induce more fusogenic activity than pNL4-3-derived Env.

Determination of a key amino acid in gp41 associated with the fusion activity. To further facilitate an accurate comparison of the abilities of the *env* genes derived from each of these isolates to support syncytium formation, we recombined three different regions in gp41 by utilizing conserved HindIII and BamHI restriction enzyme sites and newly introduced BlpI and NotI sites on gp41. The resultant viruses were analyzed in the syncytium-formation assay. As shown in Fig. 2A, NL-LAIgp41-1 and NL-L2gp41-1, carrying BlpI-HindIII fragments of pLAI and pL2, were able to reproduce the highly fusogenic activity observed in the LAIgp160, LAIgp41, L2gp160, and L2gp41 viruses. Thus, we found that the fusogenic activity of L2/LAI viruses was determined by an amino-terminal domain of gp41.

To identify the determinant of the syncytium-forming activity at the amino acid level, we performed site-directed mutagenesis. Since the amino-terminal domain of gp41 of pLAI or pL2 harbors three or four different amino acids, respectively (two amino acid differences are common in both clones), a total of five amino acid changes were introduced into pNL4-3: 21C→A (common in pLAI and pL2), 22T→R (pLAI type), 22T→A (pL2), 36D→G (common in pLAI and pL2), and 91L→F (pL2) of gp41; the constructs were designated pNL-gp41-C21A, -T22R, -T22A, -D36G, and -L91F, respectively. As shown in Fig. 2B, only the D36G mutation, which is common between L2 and LAI, led to syncytium formation. No significant difference in the Env gp120 and gp41 protein expression was observed among all viruses tested here (data not shown). Importantly, this activity was correlated with enhancement of viral infectivity (~5.5-fold [Fig. 2C]). We therefore conclude that the single amino acid substitution 36D→G is sufficient for the altered syncytium formation activity. This was surprising since we originally sought to identify the determinants of L2-specific fusion activity. Instead, we found that 36G of gp41 is well conserved among nearly all HIV-1 isolates according to the HIV-1 sequence database and that NL4-3 is rather exceptional in that gp41 harbors 36D, as reported in the T-20 studies (24, 35, 40, 42). The implications of this result are considered in Discussion.

Effect of the 36G→D mutation in a primary-isolate-derived Env. To further investigate whether these phenomena could be observed in a primary isolate, we utilized pNL-1549, encoding a primary-isolate-derived Env, in which amino acid position 36 of gp41 is glycine. We constructed the 36D version of this clone, termed pNL-1549-G36D. As shown in Fig. 3A, the mutant virus totally lost its syncytium-forming activity, while the WT virus displayed robust syncytium formation activity. Consistently, infectivity of the mutant virus showed an ~3.5-fold reduction (Fig. 3B). We therefore conclude that the effects of amino acid substitution at position 36 on syncytium formation and viral infectivity are reproduced in the primary isolate.

Effect of the D36G mutation on viral binding activity. Next, we attempted to clarify whether the effect of the D36G mutation on the syncytium formation might be regulated by viral binding activity due to an altered interaction between gp41 and gp120. Before testing this, we first quantitatively compared the difference in the fusion activity between WT NL and the D36G mutant Envs by performing a cell-cell fusion assay. In this assay, 293T cells as effector cells were transfected with Tat and Env expression plasmids, while CD4/coreceptor-expressing MAGIC5A cells as target cells were transfected with a plasmid carrying a synthetic version of rapidly responding Luc reporter gene which is driven by the HIV-1 LTR. After coculturing effector cells and target cells, fusion activity can be quantitated by measuring Tat-induced Luc activity. Transfection efficiency was normalized with renilla luciferase expression in the effec-

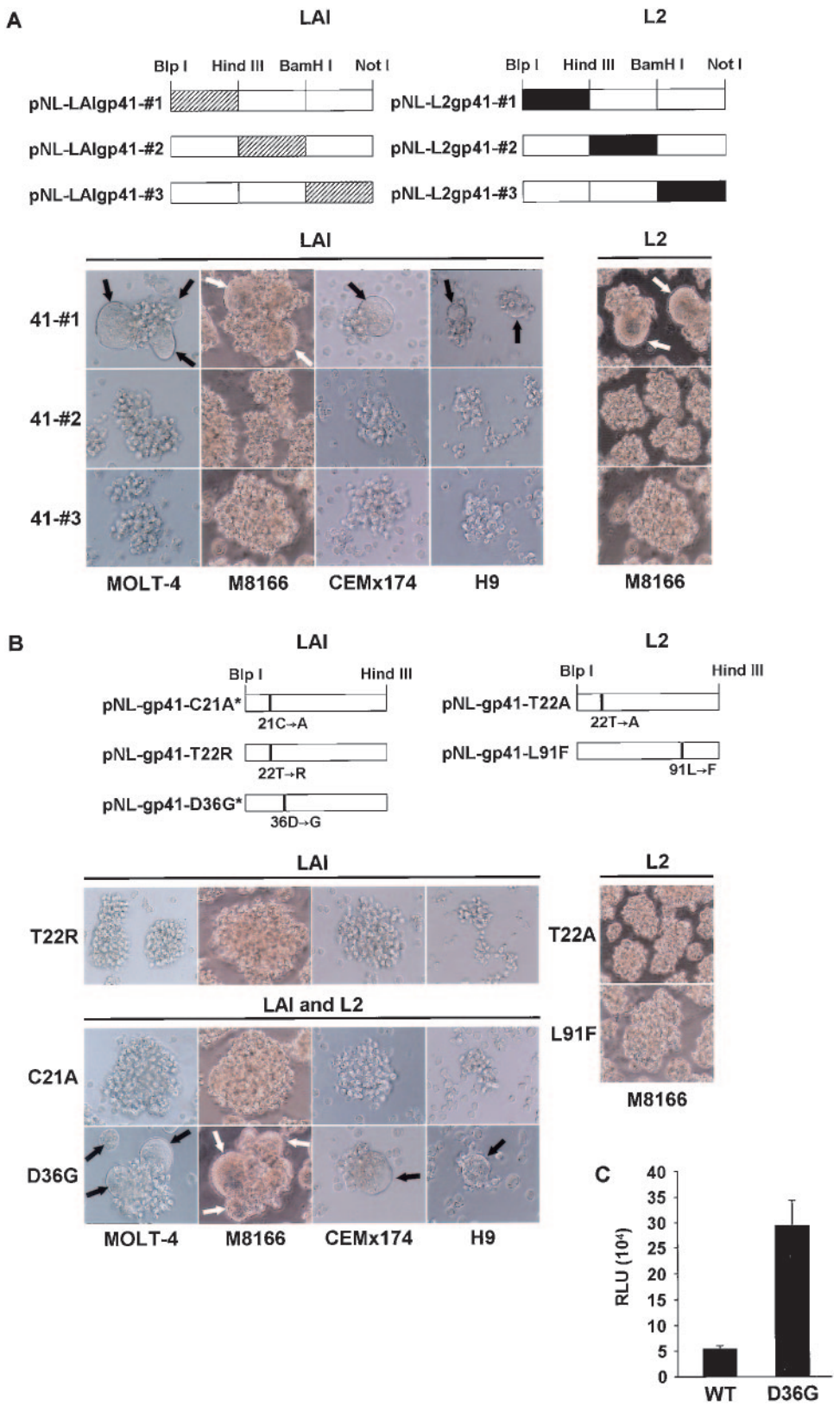

FIG. 2. Construction of gp41 recombinants and point mutants and their syncytium-forming activities and infectivities. (A) Chimeric viruses carrying three different regions of gp41 derived from pLAI or pL2 were constructed by utilizing the restriction enzyme sites BlpI, HindIII, BamHI and NotI. (B) Amino acid substitutions (21C→A, 22T→R, 22T→A, 36D→G, or 91L→F) were introduced within the BlpI-HindIII region of gp41 by site-directed mutagenesis. Asterisks show mutant constructs harboring a mutation commonly seen in both pLAI and pL2. The syncytium-formation assay (A and B) was performed as described for Fig. 1. Arrows indicate the formation of syncytia. (C) To determine infectivity, 5×10^5 MAGIC5A cells were infected with 10 ng of NL-Luc-envCT (WT) or NL-Luc-D36G (D36G), harboring the Luc gene in place of *nef*. After 48 h, cells were lysed and subjected to Luc assay. Averages from three independent experiments with standard deviations are indicated. RLU, relative light units.

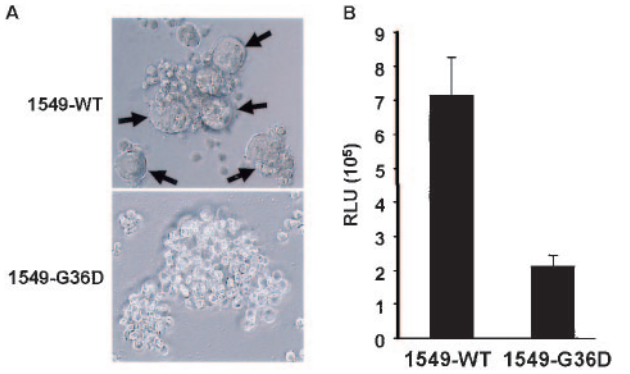

FIG. 3. Effect of the amino acid change at position 36 in gp41 in a primary-isolate-derived Env. (A) A syncytium formation assay was performed with MOLT-4 cells inoculated with NL-1549 (1549-WT) viruses carrying a primary-isolate (QH1549)-derived Env or with NL-1549-G36D (1549-G36D) viruses harboring the amino acid change 36G→D in 1549 gp41. Arrows indicate the formation of syncytia. (B) Infectivities of NL-Luc-1549 (1549-WT) and NL-Luc-1549-G36D (1549-G36D) viruses were measured by Luc assay as described for Fig. 2C. Averages from three independent experiments with standard deviations are indicated. RLU, relative light units.

tor cells, and equivalent levels of expression of WT and D36G Envs were confirmed by immunoblotting. As shown in Fig. 4A, the D36G Env enhanced Luc activity ~5-fold more than WT Env, consistent with microscopic observation of the fusion activity shown in Fig. 2B. In the viral binding assay, MAGIC5A cells were incubated with WT Env- and D36G Env-encoding viruses at 4°C, which is a temperature permissive for virus

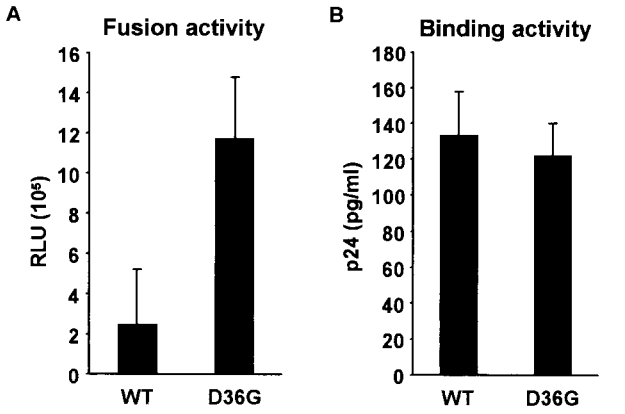

FIG. 4. Comparisons of cell-cell fusion (A) and viral binding (B) between WT and D36G mutant Envs. (A) 293T cells as the effector cells were transfected with pNLnΔBs (WT) or pNLnΔBs-D36G (D36G) and Tat expression plasmids, while MAGIC5A cells as the target cells were transfected with pLTR-hLucP+. Forty-eight hours later, both cell types were washed, trypsinized, and cocultured. After 5 h, cells were lysed and subjected to Luc assay. Averages from three independent experiments with standard deviations are indicated. RLU, relative light units. (B) MAGIC5A cells (1.5×10^6) were incubated with medium containing 100 ng of NL-Δenv, NL-envCT (WT), or NL-gp41-D36G (36G) viruses at 4°C. After 3 h, cells were extensively washed with ice-cold PBS three times and lysed with lysis buffer. Cell lysates were analyzed for p24 levels by ELISA. The background obtained with NL-Δenv viruses was subtracted from sample values. Averages from three independent experiments with standard deviations are indicated.

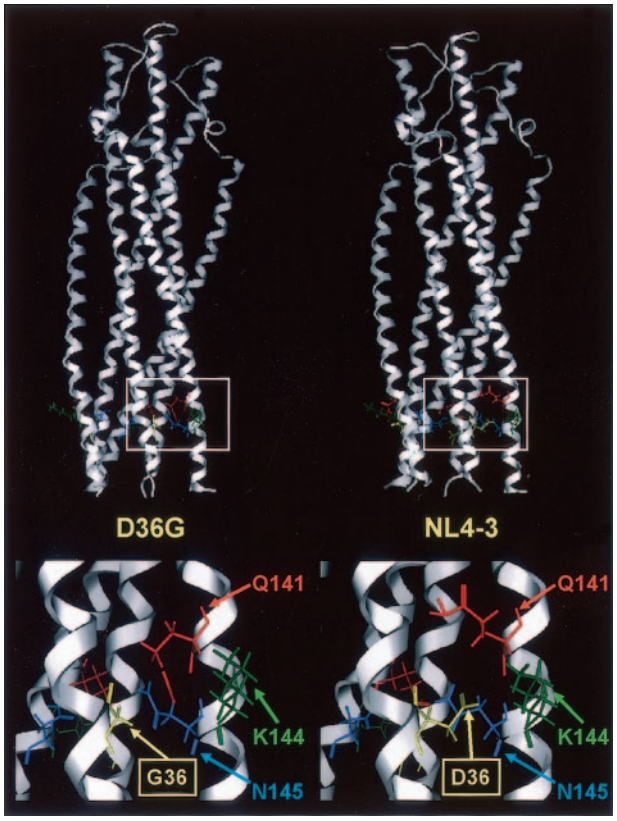

FIG. 5. Molecular modeling of HIV-1 gp41 ectodomain trimer. The 3-D model of an HIV-1 gp41 ectodomain trimer was constructed by the homology modeling technique using the MOE. HIV-1 gp41 ectodomain trimers of D36G (upper left) and NL4-3 (upper right) are displayed. Target portions of each trimer around amino acid position 36 are shown with side chains of position 36 in the N-peptide region and related amino acids within the C-peptide region. Arrows indicate the side chains of N and C helices of D36G (lower left) and NL4-3 gp41 (lower right).

binding but not internalization. After 3 h, unbound virions were removed by extensive washing, and cells were lysed and subjected to p24 ELISA. Background activity of the control virus (*env* defective), which showed ~30% of the binding activity of WT Env, was subtracted from the activity obtained for WT and D36G Envs. As shown in Fig. 4B, WT and D36G mutant viruses displayed equivalent levels of viral binding ability. We therefore conclude that the effect of the D36G amino acid substitution on syncytium formation results from an enhancement in fusogenic activity and not from enhanced virus binding due to an altered interaction between gp41 and gp120.

Comparison of the 3-D structure models of the gp41 ectodomain trimer. To more fully understand the mechanism by which fusogenicity differs between NL4-3 and the D36G mutant, we analyzed the effect of the D36G mutation on the predicted 3-D structure of the gp41 ectodomain trimer. Thermodynamically stable ectodomain structures of HIV-1 NL4-3 and its D36G mutant were constructed by homology modeling as described in Materials and Methods. As shown in Fig. 5, when the two structures were compared, it was obvious that the side chain of amino acid at position 36 in the N helix could affect the potential movement of the C helix of NL4-3 but not

that of the D36G mutant. The side chain of the aspartic acid in the NL4-3 (36D) model was shown to protrude toward the main chain of the C helix positioned in parallel with the N helix, being surrounded closely by the side chains of three amino acids in the C helix, i.e., Q141, K144, and N145. In such a structure, if the C helix moves vertically or horizontally during six-helix bundle formation, there could be a steric clash between the side chain of 36D and some of the three amino acids. In addition, the negatively charged 36D could induce distortion or incorrect positioning of the N and C helices by forming a misdirected salt bridge with K144, leading to a less stable helix structure. The positioning of the smaller, noncharged side chain of the glycine at position 36 in the D36G mutant model suggests that it would not clash with the side chains of the C helix during six-helix bundle formation. The model also predicts that the amino acid substitution at position 36 might cause a change in positioning of both the C and N helices per se. The mean distance between the main-chain backbones of the N and C helices was shorter in the D36G models than in the NL4-3 model (5.45 Å and 6.13 Å, respectively). Although the expected difference (about 0.7 Å) was in the range of RMSD between the predicted and actual structures, it was constantly observed with models made by different procedures, suggesting its intrinsic significance due to the difference of the size of side chain at position 36. Together, the data suggest that the substitution at position 36 with a charged, larger amino acid affects not only the local conformation of the helix but also the overall positioning of the two helices. Thus, the alteration of the amino acid at position 36 has a significant impact on determining the conformation of the N and C helices in the hairpin structure during membrane fusion.

DISCUSSION

In this study, we initially attempted to identify which region of the HIV-1 envelope protein could be responsible for the highly fusogenic activity that was observed in L2 viruses produced from MT-4 cells surviving after infection with LAI viruses (16, 20, 32). As a result of recombinational and mutational analyses based on pNL4-3, we found that a substitution of glycine (present in pL2/pLAI) for aspartic acid (present in pNL4-3) at position 36 of the ectodomain of gp41 was necessary and sufficient to confer robust syncytium-forming activity as well as enhanced infectivity. This phenomenon was confirmed by using a primary-isolate-derived Env protein with a glycine located at position 36 of this gp41 ectodomain. By performing quantitative fusion assays and viral binding assays, enhanced fusion activity was found not to be due to increased binding efficiency by altered gp41-mediated activity of gp120 but to be directly due to actual enhancement of viral fusion activity.

It is somewhat surprising that we could not determine any other key amino acid change which could display high fusion activity, since 36G of the gp41 ectodomain is conserved not only in pL2/pLAI but also in most other HIV-1 isolates (even in LAI/IIIB derivatives) and since one of the most widely used HIV-1 clones, pNL4-3, consisting of LAI/BRU at the 3′half, is rather exceptional, as first shown in the reports on T-20 (24, 35, 40, 42) (see below). Besides, one discrepancy remains in that although both L2 and LAI Envs harbor 36G in the ectodomain of gp41, L2 viruses are derived from the past virus stock of MT-4→MOLT-4-propagated strain LAI, which was not able to induce syncytium formation efficiently (32). It seems likely, however, that the majority of these polyclonal LAI preparations from MT-4/MOLT-4 cells might have carried 36D of gp41, which confers considerably less fusogenicity. We hypothesize that viruses carrying D36 in gp41 would take advantage of reduced fusogenic activity to lead to higher levels of viral propagation, since low-level cytopathic activity as a result of weak fusogenicity in D36 viruses might allow infected cells to survive longer than would G36 viruses. In terms of viral infectivity, D36 viruses should retain low but sufficient infectivity, as NL4-3 does. We therefore assume that D36 viruses might have dominated polyclonal LAI preparations from MT-4/MOLT-4 during the establishment of persistently infected cells. On the other hand, the reason why, despite the acquisition of high fusogenicity, L2-producing cells could survive after the in vitro acute phase of infection (20) might be that produced virions are replication defective because of the mutation in the protease gene and that the virus-producing cells have down-regulated CD4 from the cell surface, not allowing L2 virions to superinfect the cells.

The accuracy of the homology modeling is highly dependent on resolution of template structure for the modeling, as well as the degree of sequence similarity between the template and target proteins (2, 39). To obtain a high-quality gp41 ectodomain model, we used the 1QBZ structure, which was determined by X-ray crystallography analysis to have the best resolution (1.47 Å) and is the most accurate and complete structure of a retroviral gp41 ectodomain determined to date (48). Furthermore, 1QBZ has a sequence similarity of 52.5% to the target NL4-3 gp41 ectodomain, which is high enough to construct high-accuracy models with RMSDs of ~1 Å for the main chain between predicted and actual structures (2). Therefore, the gp41 ectodomain models presented here are likely to be highly accurate, predicting the six-helix bundle structure of each strain with an RSMD of ~1 Å for the main chain.

The comparison of the six-helix bundle models of NL4-3 and the D36G mutant revealed notable structural differences around amino acid position 36, which potentially the affect ability of the ectodomain to induce conformational change (Fig. 5). The models suggest that the NL4-3 ectodomain can be more refractory to the conformational changes than the D36G mutant ectodomain, because of more efficient steric clash and coulomb interaction between the N and C helix side chains (Fig. 5). This prediction is consistent with the experimental data indicating that the NL4-3 gp41 is less fusogenic than the gp41 with the D36G substitution (Fig. 1 to 4). Together, our data suggest that the amino acid at position 36 in the N helix is a critical regulator for the structural changes of the ectodomain.

Figure 6 shows a model of HIV-1 membrane fusion and the difference in fusion efficiency between 36D and 36G Envs. Binding of gp120 to CD4 and a chemokine receptor (not shown) leads to a conformational change in gp120 that alters the interactions of gp120 with gp41. This allows the gp41 fusion peptide to be exposed and to insert into the target cell membrane (Fig. 6, upper left) and allows the N-peptide region to form an exposed trimeric coiled coil and the C-peptide region to be exposed as well (prehairpin intermediate shown in Fig. 6,

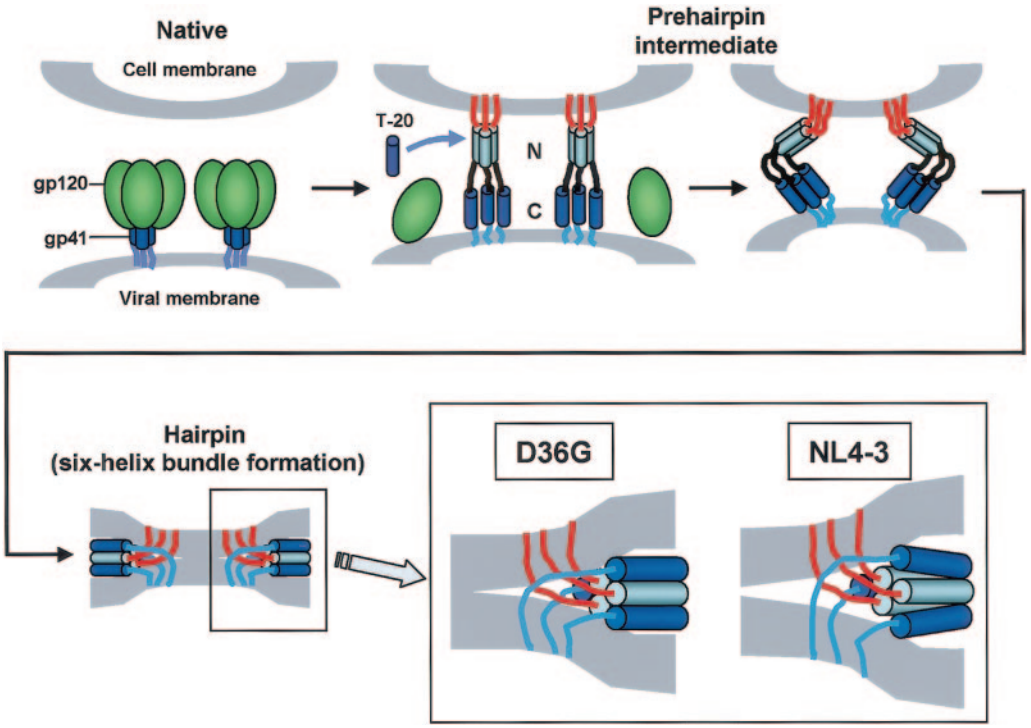

FIG. 6. A model of the HIV-1 Env-mediated fusion mechanism and a putative difference in hairpin formation between D36G and NL4-3 Envs. This model is adapted from that of Koshiba and Chan (22). Binding of gp120 to CD4 and a coreceptor (not shown) induces a conformational change in gp120 that allows exposure of gp41 fusion peptide (red) and its penetration into the target cellular membrane and allows the formation of the prehairpin intermediate (upper panel). As shown in the lower left panel, hairpin (six-helix bundle) formation occurs between trimeric N-peptide (gray) and C-peptide (blue) regions. Enlargements of putative six-helix bundles of D36G and NL4-3 gp41 ectodomains are displayed in the lower right panel.

upper middle and right). This intermediate is relatively long-lived and is vulnerable to C-peptide inhibitors such as T-20. When the C-peptide region is brought into close proximity to the N-peptide coiled coil and adopts a helical conformation, the prehairpin intermediate resolves to the fusion-active hairpin structure, which is a coiled coil composed of internal triple-stranded N-peptide helices paired with antiparallel outer C-peptide helices packed along hydrophobic grooves, forming a six-helix bundle. This rearrangement results in membrane apposition (Fig. 6, lower left). As shown in the lower right panel of Fig. 6, while the D36G mutant, which can be considered a consensus gp41, undergoes the normal six-helix bundle formation, NL4-3 carrying 36D in gp41 faces physical impediments to this formation since the protrusion of the negatively charged 36D residue in the N helix toward the C helix would induce a steric clash between the N and C helices, a salt bridge with 36D and K144 in the C helix, and an extended distance between the main-chain backbones of the N and C helices.

T-20 is a 36-amino-acid synthetic peptide that is homologous to the last 36 amino acids of the C-peptide helix (8, 27, 45) in the ectodomain of gp41. By competitively binding the N-peptide helix (Fig. 6, upper middle), T-20 blocks formation of the hairpin structure necessary for membrane fusion. Studies in vitro have shown that T-20 prevents cell-free HIV-1 infection and virus-mediated cell-cell fusion (35, 40). After in vitro passage in the presence of increasing concentrations of T-20, resistant variants of HIV-1_{IIIB} developed mutations at positions 36 and 38 (G to D or S and V to M) (35). Also, sequence analysis in vivo indicated that T-20-resistant viruses frequently and specifically contained mutations at position 36 (G to D), leading to a marked decrease in susceptibility to T-20 inhibition (42). These findings were supported by mutational evidence that compared with NL-D36G viruses (NL4-3 altered to match the consensus sequence at position 36), native NL4-3 (36D) displayed eightfold reduction in T-20 sensitivity (17). This is intriguing in that the position of the mutation observed in the T-20 escape mutants is exactly equivalent to that of the target mutation in our study. Just as observed in our experiments, the mutation which naturally occurs in the viruses escaping from T-20 is expected to induce a reduction in fusion activity, but the mutants still retain infectibility as high as that of NL4-3 viruses. Our findings, therefore, imply that the phenotypic and structural differences between fusogenic and nonfusogenic viruses described in this paper may reflect those between T-20-sensitive and nonsensitive viruses and furthermore suggest that the 36D mutation observed in T-20-resistant mutants might reduce the T-20 binding efficiency by the same mechanism as discussed above.

Considerable work on gp41 through mutagenesis studies and escape variants arising from T-20 selective pressure with the alterations in virus replication kinetics has indicated that other positions of gp41 also regulate the fusogenicity. Among gp41 mutants reported so far, many of the gp41 mutations leading to reduced fusion activity are located within or in the proximity of the "deep pocket" (6), such as L54, L55, L57, V59, W60, G61, I62, W117, W120, and I124 (4, 9, 11, 14, 25, 34, 41, 44). Since

the mutations of these conserved residues required for the six-helix bundle formation abolish viral replication (29), this pocket could be a good target for T-1249, the second fusion inhibitor, whose binding region extends into the deep pocket (13). The W85M mutation, located in the side of disulfide-bonded loop, confers impaired fusogenicity but wild-type infectivity (4). Among several mutations which have been reported to impair the fusogenicity and are located in the T-20 target region, such as I37, Q40, L45, and I48 (4, 8, 14, 25), naturally occurring mutations in the presence of T-20 are found in I37 and L45 in addition to G36 (whose phenotype was first described in this study). Fusion phenotypes of other mutants seen in T-20 resistance in vivo and in vitro (Q32, V38, and Q39) are undetermined (27, 28, 35, 42).

In conclusion, our data indicate that amino acid 36 in the gp41 ectodomain, which is conserved in nearly all HIV-1 isolates except for NL4-3 and T-20 escape viruses, controls the fusogenic activity and that structural impediment in the gp41 ectodomain of NL4-3 and T-20 escape viruses may lead to the inefficient membrane fusion. Further studies will be required to fully understand the mechanism by which viruses acquire resistance to the T-20 fusion inhibitor.

ACKNOWLEDGMENTS

We are grateful to David Chan for giving us permission to use and modify Fig. 6 and for critical reading of the manuscript, to Bryan R. Cullen for helpful discussion, and to Masashi Tatsumi for providing MAGIC5A cells.

This work was supported in part by a grant from the Ministry of Education, Science, Technology, Sports and Culture of Japan and by a grant from the Ministry of Health, Labor and Welfare of Japan.

REFERENCES

1. **Adachi, A., H. E. Gendelman, S. Koenig, T. Folks, R. Willey, A. Rabson, and M. A. Martin.** 1986. Production of acquired immunodeficiency syndrome-associated retrovirus in human and nonhuman cells transfected with an infectious molecular clone. J. Virol. **59:**284–291.
2. **Baker, D., and A. Sali.** 2001. Protein structure prediction and structural genomics. Science **294:**93–96.
3. **Caffrey, M., M. Cai, J. Kaufman, S. J. Stahl, P. T. Wingfield, D. G. Covell, A. M. Gronenborn, and G. M. Clore.** 1998. Three-dimensional solution structure of the 44 kDa ectodomain of SIV gp41. EMBO J. **17:**4572–4584.
4. **Cao, J., L. Bergeron, E. Helseth, M. Thali, H. Repke, and J. Sodroski.** 1993. Effects of amino acid changes in the extracellular domain of the human immunodeficiency virus type 1 gp41 envelope glycoprotein. J. Virol. **67:**2747–2755.
5. **Cao, J., B. Vasir, and J. G. Sodroski.** 1994. Changes in the cytopathic effects of human immunodeficiency virus type 1 associated with a single amino acid alteration in the ectodomain of the gp41 transmembrane glycoprotein. J. Virol. **68:**4662–4668.
6. **Chan, D. C., D. Fass, J. M. Berger, and P. S. Kim.** 1997. Core structure of gp41 from the HIV envelope glycoprotein. Cell **89:**263–273.
7. **Chan, D. C., and P. S. Kim.** 1998. HIV entry and its inhibition. Cell **93:**681–684.
8. **Chen, C. H., T. J. Matthews, C. B. McDanal, D. P. Bolognesi, and M. L. Greenberg.** 1995. A molecular clasp in the human immunodeficiency virus (HIV) type 1 TM protein determines the anti-HIV activity of gp41 derivatives: implication for viral fusion. J. Virol. **69:**3771–3777.
9. **Chen, S. S., C. N. Lee, W. R. Lee, K. McIntosh, and T. H. Lee.** 1993. Mutational analysis of the leucine zipper-like motif of the human immunodeficiency virus type 1 envelope transmembrane glycoprotein. J. Virol. **67:**3615–3619.
10. **Decroly, E., M. Vandenbranden, J. M. Ruysschaert, J. Cogniaux, G. S. Jacob, S. C. Howard, G. Marshall, A. Kompelli, A. Basak, F. Jean, and et al.** 1994. The convertases furin and PC1 can both cleave the human immunodeficiency virus (HIV)-1 envelope glycoprotein gp160 into gp120 (HIV-1 SU) and gp41 (HIV-I TM). J. Biol. Chem. **269:**12240–12247.
11. **Dubay, J. W., S. J. Roberts, B. Brody, and E. Hunter.** 1992. Mutations in the leucine zipper of the human immunodeficiency virus type 1 transmembrane glycoprotein affect fusion and infectivity. J. Virol. **66:**4748–4756.
12. **Dubay, J. W., S. J. Roberts, B. H. Hahn, and E. Hunter.** 1992. Truncation of the human immunodeficiency virus type 1 transmembrane glycoprotein cytoplasmic domain blocks virus infectivity. J. Virol. **66:**6616–6625.
13. **Eron, J. J., R. M. Gulick, J. A. Bartlett, T. Merigan, R. Arduino, J. M. Kilby, B. Yangco, A. Diers, C. Drobnes, R. DeMasi, M. Greenberg, T. Melby, C. Raskino, P. Rusnak, Y. Zhang, R. Spence, and G. D. Miralles.** 2004. Short-term safety and antiretroviral activity of T-1249, a second-generation fusion inhibitor of HIV. J. Infect. Dis. **189:**1075–1083.
14. **Follis, K. E., S. J. Larson, M. Lu, and J. H. Nunberg.** 2002. Genetic evidence that interhelical packing interactions in the gp41 core are critical for transition of the human immunodeficiency virus type 1 envelope glycoprotein to the fusion-active state. J. Virol. **76:**7356–7362.
15. **Freed, E. O., D. J. Myers, and R. Risser.** 1990. Characterization of the fusion domain of the human immunodeficiency virus type 1 envelope glycoprotein gp41. Proc. Natl. Acad. Sci. USA **87:**4650–4654.
16. **Goto, T., K. Ikuta, J. J. Zhang, C. Morita, K. Sano, M. Komatsu, H. Fujita, S. Kato, and M. Nakai.** 1990. The budding of defective human immunodeficiency virus type 1 (HIV-1) particles from cell clones persistently infected with HIV-1. Arch. Virol. **111:**87–101.
17. **Greenberg, M. L., and N. Cammack.** 2004. Resistance to enfuvirtide, the first HIV fusion inhibitor. J. Antimicrob. Chemother. **54:**333–340.
18. **Hallenberger, S., V. Bosch, H. Angliker, E. Shaw, H. D. Klenk, and W. Garten.** 1992. Inhibition of furin-mediated cleavage activation of HIV-1 glycoprotein gp160. Nature **360:**358–361.
19. **Helseth, E., U. Olshevsky, D. Gabuzda, B. Ardman, W. Haseltine, and J. Sodroski.** 1990. Changes in the transmembrane region of the human immunodeficiency virus type 1 gp41 envelope glycoprotein affect membrane fusion. J. Virol. **64:**6314–6318.
20. **Ikuta, K., C. Morita, M. Nakai, N. Yamamoto, and S. Kato.** 1988. Defective human immunodeficiency virus (HIV) particles produced by cloned cells of HTLV-I-carrying MT-4 cells persistently infected with HIV. Jpn. J. Cancer Res. **79:**418–423.
21. **Kinomoto, M., T. Mukai, Y. G. Li, Y. Iwabu, J. Warachit, J. A. Palacios, M. S. Ibrahim, S. Tsuji, T. Goto, and K. Ikuta.** 2004. Enhancement of human immunodeficiency virus type 1 infectivity by replacing the region including Env derived from defective particles with an ability to form particle-mediated syncytia in CD4+T cells. Microbes Infect. **6:**911–918.
22. **Koshiba, T., and D. C. Chan.** 2003. The prefusogenic intermediate of HIV-1 gp41 contains exposed C-peptide regions. J. Biol. Chem. **278:**7573–7579.
23. **Kwong, P. D., R. Wyatt, J. Robinson, R. W. Sweet, J. Sodroski, and W. A. Hendrickson.** 1998. Structure of an HIV gp120 envelope glycoprotein in complex with the CD4 receptor and a neutralizing human antibody. Nature **393:**648–659.
24. **Lu, J., P. Sista, F. Giguel, M. Greenberg, and D. R. Kuritzkes.** 2004. Relative replicative fitness of human immunodeficiency virus type 1 mutants resistant to enfuvirtide (T-20). J. Virol. **78:**4628–4637.
25. **Lu, M., M. O. Stoller, S. Wang, J. Liu, M. B. Fagan, and J. H. Nunberg.** 2001. Structural and functional analysis of interhelical interactions in the human immunodeficiency virus type 1 gp41 envelope glycoprotein by alanine-scanning mutagenesis. J. Virol. **75:**11146–11156.
26. **Malashkevich, V. N., D. C. Chan, C. T. Chutkowski, and P. S. Kim.** 1998. Crystal structure of the simian immunodeficiency virus (SIV) gp41 core: conserved helical interactions underlie the broad inhibitory activity of gp41 peptides. Proc. Natl. Acad. Sci. USA **95:**9134–9139.
27. **Matthews, T., M. Salgo, M. Greenberg, J. Chung, R. DeMasi, and D. Bolognesi.** 2004. Enfuvirtide: the first therapy to inhibit the entry of HIV-1 into host CD4 lymphocytes. Nat. Rev. Drug Discov. **3:**215–225.
28. **Menzo, S., A. Castagna, A. Monachetti, H. Hasson, A. Danise, E. Carini, P. Bagnarelli, A. Lazzarin, and M. Clementi.** 2004. Genotype and phenotype patterns of human immunodeficiency virus type 1 resistance to enfuvirtide during long-term treatment. Antimicrob. Agents Chemother. **48:**3253–3259.
29. **Mo, H., A. K. Konstantinidis, K. D. Stewart, T. Dekhtyar, T. Ng, K. Swift, E. D. Matayoshi, W. Kati, W. Kohlbrenner, and A. Molla.** 2004. Conserved residues in the coiled-coil pocket of human immunodeficiency virus type 1 gp41 are essential for viral replication and interhelical interaction. Virology **329:**319–327.
30. **Mochizuki, N., N. Otsuka, K. Matsuo, T. Shiino, A. Kojima, T. Kurata, K. Sakai, N. Yamamoto, S. Isomura, T. N. Dhole, Y. Takebe, M. Matsuda, and M. Tatsumi.** 1999. An infectious DNA clone of HIV type 1 subtype C. AIDS Res. Hum. Retroviruses **15:**1321–1324.
31. **Morikawa, Y., E. Barsov, and I. Jones.** 1993. Legitimate and illegitimate cleavage of human immunodeficiency virus glycoproteins by furin. J. Virol. **67:**3601–3604.
32. **Ohki, K., Y. Kishi, Y. Nishino, M. Sumiya, T. Kimura, T. Goto, M. Nakai, and K. Ikuta.** 1991. Noninfectious doughnut-shaped human immunodeficiency virus type 1 can induce syncytia mediated by fusion of the particles with CD4-positive cells. J. Acquir. Immune Defic. Syndr. **4:**1233–1240.
33. **Owens, R. J., C. Burke, and J. K. Rose.** 1994. Mutations in the membrane-spanning domain of the human immunodeficiency virus envelope glycoprotein that affect fusion activity. J. Virol. **68:**570–574.
34. **Perrin, C., E. Fenouillet, and I. M. Jones.** 1998. Role of gp41 glycosylation sites in the biological activity of human immunodeficiency virus type 1 envelope glycoprotein. Virology **242:**338–345.

35. **Rimsky, L. T., D. C. Shugars, and T. J. Matthews.** 1998. Determinants of human immunodeficiency virus type 1 resistance to gp41-derived inhibitory peptides. J. Virol. **72:**986–993.
36. **Tan, K., J. Liu, J. Wang, S. Shen, and M. Lu.** 1997. Atomic structure of a thermostable subdomain of HIV-1 gp41. Proc. Natl. Acad. Sci. USA **94:** 12303–12308.
37. **Tokunaga, K., M. L. Greenberg, M. A. Morse, R. I. Cumming, H. K. Lyerly, and B. R. Cullen.** 2001. Molecular basis for cell tropism of CXCR4-dependent human immunodeficiency virus type 1 isolates. J. Virol. **75:**6776–6785.
38. **Tokunaga, K., A. Kojima, T. Kurata, K. Ikuta, H. Akari, A. H. Koyama, M. Kawamura, R. Inubushi, R. Shimano, and A. Adachi.** 1998. Enhancement of human immunodeficiency virus type 1 infectivity by Nef is producer cell-dependent. J. Gen. Virol. **79:**2447–2453.
39. **Tramontano, A.** 1998. Homology modeling with low sequence identity. Methods **14:**293–300.
40. **Trivedi, V. D., S. F. Cheng, C. W. Wu, R. Karthikeyan, C. J. Chen, and D. K. Chang.** 2003. The LLSGIV stretch of the N-terminal region of HIV-1 gp41 is critical for binding to a model peptide, T20. Protein Eng. **16:**311–317.
41. **Wang, S., J. York, W. Shu, M. O. Stoller, J. H. Nunberg, and M. Lu.** 2002. Interhelical interactions in the gp41 core: implications for activation of HIV-1 membrane fusion. Biochemistry **41:**7283–7292.
42. **Wei, X., J. M. Decker, H. Liu, Z. Zhang, R. B. Arani, J. M. Kilby, M. S. Saag, X. Wu, G. M. Shaw, and J. C. Kappes.** 2002. Emergence of resistant human immunodeficiency virus type 1 in patients receiving fusion inhibitor (T-20) monotherapy. Antimicrob. Agents Chemother. **46:**1896–1905.
43. **Weissenhorn, W., A. Dessen, S. C. Harrison, J. J. Skehel, and D. C. Wiley.** 1997. Atomic structure of the ectodomain from HIV-1 gp41. Nature **387:** 426–430.
44. **Weng, Y., and C. D. Weiss.** 1998. Mutational analysis of residues in the coiled-coil domain of human immunodeficiency virus type 1 transmembrane protein gp41. J. Virol. **72:**9676–9682.
45. **Wild, C. T., D. C. Shugars, T. K. Greenwell, C. B. McDanal, and T. J. Matthews.** 1994. Peptides corresponding to a predictive alpha-helical domain of human immunodeficiency virus type 1 gp41 are potent inhibitors of virus infection. Proc. Natl. Acad. Sci. USA **91:**9770–9774.
46. **Willey, R. L., J. S. Bonifacino, B. J. Potts, M. A. Martin, and R. D. Klausner.** 1988. Biosynthesis, cleavage, and degradation of the human immunodeficiency virus 1 envelope glycoprotein gp160. Proc. Natl. Acad. Sci. USA **85:**9580–9584.
47. **Wu, L., N. P. Gerard, R. Wyatt, H. Choe, C. Parolin, N. Ruffing, A. Borsetti, A. A. Cardoso, E. Desjardin, W. Newman, C. Gerard, and J. Sodroski.** 1996. CD4-induced interaction of primary HIV-1 gp120 glycoproteins with the chemokine receptor CCR-5. Nature **384:**179–183.
48. **Yang, Z. N., T. C. Mueser, J. Kaufman, S. J. Stahl, P. T. Wingfield, and C. C. Hyde.** 1999. The crystal structure of the SIV gp41 ectodomain at 1.47 A resolution. J. Struct. Biol. **126:**131–144.